

CWRU-P2-94

January 1994

REFINED BIG BANG NUCLEOSYNTHESIS  
CONSTRAINTS ON  $\Omega_{Baryon}$  and  $N_\nu$ Peter J. Kernan and Lawrence M. Krauss<sup>1</sup>

*Department of Physics*  
*Case Western Reserve University*  
*10900 Euclid Ave., Cleveland, OH 44106-7079*

**Abstract**

We include correlations between elemental abundances in a Monte Carlo statistical analysis of BBN predictions, which, along with updated reaction rates and an improved BBN code, lead to tightened constraints on  $\Omega_B$  and  $N_\nu$ . Observational upper limits on the primordial  $^4\text{He}$  and  $\text{D} + ^3\text{He}$  fractions of 24% (by weight) and  $10^{-4}$  respectively lead to the limits:  $0.015 \leq \Omega_B \leq 0.070$ , and  $N_\nu \leq 3.04$ . The former limit appears to be incompatible with purely baryonic galactic halo dark matter, while the latter puts qualitatively new constraints on neutrinos, and physics beyond the standard model.

---

<sup>1</sup>Also Dept of Astronomy

The remarkable agreement, both qualitative and quantitative, of the predicted primordial light element abundances and those inferred from present observations yields some of the strongest evidence in favor of a homogeneous FRW Big Bang cosmology. Because of this, significant efforts have taken place over 20 years to refine BBN predictions, and the observational constraints they are related to. Several factors have contributed to the maturing of this field, including the incorporation of elements beyond  ${}^4\text{He}$  in comparison between theory and observation (i.e. [1]), and more recently: an updated BBN code [2], a more accurate measured neutron half life[3], new estimates of the actual primordial  ${}^4\text{He}$ ,  $D+{}^3\text{He}$ , and  ${}^7\text{Li}$  abundances [4, 5], and finally the determination of BBN uncertainties via Monte Carlo analysis [6]. All of these, when combined together [7] yield a consistent picture of homogeneous BBN which is at the same time strongly constrained by observation.

We have returned to re-analyze BBN constraints motivated by three factors: new measurements of

several BBN reactions, the development of an improved BBN code, and finally the realization that a correct statistical determination of BBN predictions should include correlations between the different elemental abundances. Each serves to further restrict the allowed range of the relevant cosmological observables  $\Omega_{Baryon}$  and  $N_\nu$ .

**1. New BBN Reaction Rates:** By far the most accurately measured BBN input parameter is the neutron half-life, which governs the strength of the weak interaction which interconverts neutrons and protons, and which in turn helps govern when this reaction drops out of equilibrium. Since this effectively determines the abundance of free neutrons at the onset of BBN, it

is crucial in determining the remnant abundance of  ${}^4\text{He}$ . With the advent of neutron trapping, the uncertainty in the neutron half-life quickly dropped to less than 0.5% by 1990. Nevertheless, it is the uncertainty in this parameter that governs the uncertainty in the predicted  ${}^4\text{He}$  abundance. The world average for the neutron half-life is now  $\tau_N = 889 \pm 2.1\text{sec}$  [3], which has an uncertainty which is almost twice as small as that used in previous published BBN analyses [4, 6, 7]. We utilize the updated value in our analysis.

Next, a recent measurement of

${}^7\text{Be} + p \rightarrow \gamma + {}^8\text{B}$  suggests[8] a rate about 20% smaller at low energies than previous estimates. One might expect that at high values of

$\eta_{10}$  (defined by the relation  $\Omega_B = .0036h^{-2}(T/2.726)^3\eta_{10} \times 10^{10}$ , where  $T$  is the microwave background temperature today, and  $h$  defines the Hubble parameter by  $H = 100h \text{ km}/(\text{Mpc sec})$ ) lowering this rate would result in less  ${}^7\text{Be}$  destruction, which would increase the  ${}^7\text{Li}$  abundance resulting from the decay of  ${}^7\text{Be}$  after BBN. However, this is a subdominant destruction process for  ${}^7\text{Be}$ .

We find that the reducing the rate by 20% in our code alters the remnant  ${}^7\text{Li}$  abundance by less than one part in  $10^5$ !

Outside of these, we updated the Kawano code to use the reaction rates and uncertainties from in Smith *et al* [7].

**2. New BBN Monte Carlo:** Because of the new importance of small corrections to the  ${}^4\text{He}$  abundance when comparing BBN predictions and observations, increased attention has been paid recently to effects which may alter this abundance at the 1% level or less. In our BBN Code several such effects were incorporated, resulting in an  $\eta_{10}$  -independent correction of +.0006

to the lowest order value of  $Y_p$  (the  ${}^4\text{He}$  mass fraction). This is a change of  $+.0031$  compared to the value used in previous published analyses[4, 6, 7].

This earlier value was based on correcting the lowest order value of  $Y_p$  by an amount  $-.0025$  [2], based on the work of Dicus *et al* [9]. The Dicus *et al* correction has two significant pieces:  $-.0013$  from integrating the weak rates rather than using an expansion in powers of  $T$  to calculate  $\lambda(n \leftrightarrow p)$ , and  $-.0009$  from using the correct Coulomb correction, rather than simply scaling the neutron lifetime. This latter approximation

incorrectly “Coulomb corrects” rates which do not feel the electromagnetic potential, such as  $ne^+ \rightarrow p\bar{\nu}$ , and also ignores any temperature dependence. The remaining corrections — radiative, finite temperature, electron mass effects and neutrino heating—either

effectively cancel (the first two) or are insignificant (the last two) [9].

In the present code, more than half of the new correction

is due to finer integration of the nuclear abundances. Making the time-step in the code short enough that different Runge-Kutta drivers result in the same number for the  ${}^4\text{He}$  abundance produces a nearly  $\eta_{10}$  independent change in  $Y_p$  of  $+.0017$  [10]. The other major change is the inclusion of  $M_N^{-1}$  effects[11]. Seckel showed that the effects on the weak rates due to nucleon recoil, weak magnetism, thermal motion of the nucleon target and time dilation of the neutron lifetime combine to increase  $Y_p$  by  $\sim .0012$ .

The kinematics of nuclear recoil, are responsible for roughly

25% of the increase which Seckel found [10]. Also included in the correction is an small increase of  $.0002$  in  $Y_p$  from momentum dependent neutrino decoupling [12, 13].

Finally, we have utilized a Monte Carlo procedure in order to incorporate existing uncertainties and determine confidence limits on parameters. Such a procedure was first carried out by Krauss and Romanelli [6], who chose the BBN reaction rates from a (temperature-independent) distribution based on then existing experimental uncertainties. Their procedure was further refined by Smith et al [7], who both updated the experimental uncertainties, and utilized temperature dependent uncertainties in their analysis. Here we utilized the nuclear reaction rate uncertainties quoted by Smith et al (including the temperature dependent uncertainties for  ${}^3\text{He}(\alpha, \gamma){}^7\text{Be}$  and  ${}^3\text{H}(\alpha, \gamma){}^7\text{Li}$ ) except for the updated reactions described earlier. Each reaction rate was determined using a Gaussian distributed random variable centered on unity, with a width based on the quoted  $1 - \sigma$  uncertainty from Smith *et al*. For the

rates without temperature dependent uncertainties this number was used as a multiplier

throughout the nuclear abundance integration. For the two rates with temperature dependent uncertainties the original uniformly distributed random number was saved and mapped into a new gaussian

distribution with the appropriate width at each time step.

While the Smith *et al* analysis cut off each distribution at  $\pm 2.6\sigma$ , we did not make such a restriction. Our code was designed to generate warnings, discard data, and reset random numbers if reaction rate values which were generated became nonsensical (i.e. negative). Warnings were generated only for the temperature dependent rates. For  ${}^3\text{H}(\alpha, \gamma){}^7\text{Li}$  1 warning per 4000 BBN runs was generated, less than 1 warning per 30000 runs was generated

for  ${}^3\text{He}(\alpha, \gamma){}^7\text{Be}$ .

The results of our updated BBN Monte Carlo analysis are displayed in figure 1, where the symmetric 95% confidence level predictions for each elemental abundance are plotted. Also shown are claimed upper limits for each of the light elements [4, 5, 7] based on

observation<sup>2</sup>. This figure also allows one to assess the significance of the size of the corrections we have used in relation to the width of the 95% C.L. band for  $Y_p$ , which turns out to be  $\sim .002$ . The total change in  $Y_p$  of  $\approx +.003$  from previous BBN analyses conspires with the reduced uncertainty in the neutron lifetime, which narrows the uncertainty in  $Y_p$  and also feeds into the uncertainties in the other light elements, to reduce the acceptable range where the predicted BBN abundances are consistent with the inferred primordial abundances.

**3. Statistical Correlations Between Predicted Abundances:** While the introduction of a Monte Carlo procedure was a significant improvement in the evaluation of BBN uncertainties and predictions, the determination of limits on the allowed range of BBN parameters  $\Omega_{baryon}$  and  $N_\nu$  based on comparison of symmetric 95% confidence limits for single elemental abundances with observations, as has become the standard procedure, overestimates the allowed range. This is because the BBN reaction network ties together all reactions, so that the predicted elemental abundances are not statistically independent. In addition, the use of symmetric confidence limits is too conservative. Addressing both of these factors is a central feature of our work.

Figure 2 displays the locus of predicted values for the fractions  $Y_p$  and

---

<sup>2</sup>Where the estimates differ, we have used the more conservative one.

D +<sup>3</sup>He/H for 1000 BBN models generated from the distributions described above for  $\eta_{10} = 2.71$  (figure a) and  $\eta_{10} = 3.08$  (figure b). Also shown is the  $\chi^2 = 4$  joint confidence level contour derived from this distribution, in a Gaussian approximation, calculating variances and covariances in the standard manner. The horizontal and vertical tangents to this contour correspond to the individual symmetric  $\pm 2\sigma$  limits on Gaussianly distributed  $x$  and  $y$  variables. As can be seen, the distribution is close to Gaussian, but has deviations. Nevertheless, this approximation is useful to quantify the magnitude of correlations and variances. We calculated the normalized covariance matrices at different values of  $\eta_{10}$ , and display the covariances in Table 1. As is evident from this table, as well as the figure, and as is also well known on the basis of analytical arguments, there is a strong anti-correlation between  $Y_p$  and the remnant D +<sup>3</sup>He abundance. Thus, those models where <sup>4</sup>He is lower than the mean, and which therefore may be allowed by the existing quoted upper bound of 24% on  $Y_p$ , will also generally produce a larger remnant D+<sup>3</sup>He/H abundance, which can be in conflict with the quoted upper bound on this combination of  $10^{-4}$ . This will have the effect of reducing the parameter space which is consistent with both limits, as we now describe.

Because our Monte Carlo generates the actual distribution of abundances, Gaussian or not, we determine a 95% confidence limit on the allowed range of  $\eta_{10}(N_\nu)$  by requiring that at least 50 models out of 1000 lie within the joint range bounded by both the <sup>4</sup>He and D +<sup>3</sup>He upper limits, as shown in figure 2. This is to be compared with the procedure which one would follow without considering joint probability distributions. In this case, one would simply check whether 50 models lie *either* to the right of the

D +  $^3\text{He}$  constraint for low  $\eta_{10}$  (figure a), or below the  $^4\text{He}$  constraint for high  $\eta_{10}$  (figure b). This is clearly a looser constraint than that obtained using the joint distribution. Finally, the procedure which has been used to-date, which is to check whether the symmetric  $2\sigma$  confidence limit for a single elemental abundance crosses into the allowed region gives even a looser constraint, as can be seen in figure 2a. This, after all corresponds to checking whether only 25 models lie to the right of the  $D + ^3\text{He}$  constraint for low  $\eta_{10}$  (figure a), or below the  $^4\text{He}$  constraint for high  $\eta_{10}$  (figure b).

In table 2 and figure 3 we display our results. Here we show the 95% confidence limits on  $\eta_{10}$ , as we have defined them above, and also using the looser procedures which ignore correlations. As can be seen, accounting for the correlations in the non-symmetric 95% confidence limit tightens constraints. Moreover, the impact of the procedure becomes stronger as the number of effective light neutrino species,  $N_\nu$  is increased. Greater than 3.04 effective light neutrino types is ruled out only once correlations are taken into account.

We also determined an upper limit on  $\eta_{10}$  using just  $^7\text{Li}$ . Requiring  $^7\text{Li}/H \leq 2.3 \times 10^{-10}$  [5, 7] yields a limit  $\eta_{10} \leq 5.27$ . This is weaker than the  $^4\text{He}$  limit, and there remains some debate about the actual observational upper limit on primordial  $^7\text{Li}$  (i.e. changing 2.3 to 1.4[4] will lower the limit on  $\eta_{10}$  to 4.15.). Alternatively, we can use the bound on  $\eta_{10}$  derived above to set an allowed range of  $9 \times 10^{-11} \rightarrow 1.5 \times 10^{-10}$  on the primordial values of  $^7\text{Li}$ , which should be compared with the observational estimates.

#### 4. Conclusions and Implications: The new

constraints we have derived here on  $\eta_{10}$ , and  $N_\nu$ , taken at face value, have significant implications for cosmology,

dark matter, and particle physics. The limit on  $\eta_{10}$  corresponds to the limit  $0.015 \leq \Omega_{Baryon} \leq 0.070$ . (To derive this bound we required  $0.4 \leq h \leq 0.8$ , as is required by direct measurements and

limits on the age of the universe.) Thus, *if the quoted observational upper limits on the  $Y_p$  and  $D+{}^3\text{He}/H$  are valid* homogeneous BBN implies that:

(a) The upper limit on  $\Omega_{baryon}$  seems

incompatible with all, or even galactic halo dark matter being purely baryonic.

(b) The bound on the number of effective light degrees of freedom during nucleosynthesis is *very severe*, corresponding to less than 0.04 extra light neutrinos. This is a qualitatively different constraint than the previously quoted limit of 0.3 extra neutrinos. For example, it rules out *any* Dirac mass for a neutrino without some extension of the standard model because even a right handed component which freezes out at temperatures in excess of 300 GeV will contribute in excess of 0.047 extra neutrinos during BBN i.e. [14] without extra particles

introduced whose annihilation can further suppress its abundance. Even allowing 0.047 extra light neutrinos, the upper limit on a Dirac mass would be reduced to  $\approx 5$  keV [17, 18]. Similarly, new light scalars are ruled out unless they decouple above  $300\text{GeV}$ . A  $\nu_\tau$  mass greater than 0.5 MeV with lifetime exceeding 1 sec. is also ruled out due to its effect on the expansion rate during BBN i.e. see [15, 16]. Also, neutrino interactions induced by extended technicolor at scales less than  $O(100)$  TeV are ruled out [19]. Moreover, sterile right handed neutrinos [20] would be ruled out as warm dark matter as the lower limit on their mass would now be  $O(1\text{keV})$ . ( We will explore these

constraints further in subsequent work).

Finally, having devoted considerable effort to accounting for the statistical uncertainties in BBN predictions, we must still stress that the largest, and most significant, uncertainties in the comparison of BBN predictions with observations come from the latter. Moreover, the uncertainties in these observational limits are dominated by systematic, and not statistical effects. Hence, the 95% confidence limits we derive must be qualified by the recognition that their significance is really only as good as the observational limits are. Such limits cannot, at present, be taken to imply statistically inviolate constraints on neutrino parameters or  $\Omega_B$ . In other words, systematic errors in the quoted upper limits on the inferred primordial light element abundances could allow the limits quoted here to be broadened.

Nevertheless, the theory can be carefully tested. If, for example, baryonic dark matter is found to make up the galactic halo or if neutrino mass measurements conflict with the above bounds, this would most likely imply that the quoted upper limits on  ${}^4\text{He}$ , or on  ${}^3\text{He} + D$  are flawed. This would be of great interest for stellar evolution studies.

Indeed, the existing constraints from BBN are now so tight—requiring a primordial  ${}^4\text{He}$  fraction in excess of 23.8% for consistency—that an agnostic view is prudent at the present time as to whether the constraints derived above will be satisfied or else whether observations will require revision in the inferred primordial abundance estimates. Finally, we note that inhomogeneous BBN is not likely to alter this conclusion, as recent work has established. [21].

## References

- [1] R.V. Wagoner, W.A. Fowler and F. Hoyle, *Ap. J.* **148**, 3 (1967); H. Reeves et al, *Ap. J.* **179**, 909 (1973)
- [2] L.Kawano, Fermilab-Pub-88/34-A (1988); L.Kawano, Fermilab-Pub-92/04-A (1992)
- [3] Particle Data Group, *Review of Particle Properties*, *Phys.Rev.***D45** (1992)
- [4] T.P.Walker, G.Steigman, D.N.Schramm, K.A.Olive and H-S.Kang, *Ap.J.*, **376**, 51 (1991)
- [5] C.P. Deliyannis, P. Demarque, S.D. Kawaler, L.M. Krauss and P. Romanelli, *Phys Rev. Lett.* **62**, 1583 (1989)
- [6] L.M.Krauss and P.Romanelli, *Ap.J.*, **358**, 47 (1990)
- [7] W.K.Smith, L.H.Kawano and R.A.Malaney, *Ap.J.Supp.* **85**, 219 (1993)
- [8] T.Motobayashi *et al*, Rikkyo RUP 94-2 / Yale-40609-1141 *submitted to PRL*
- [9] D.A.Dicus, E.W.Kolb, A.M.Gleeson, E.C.G.Sudarshan, V.L.Teplitz and M.S.Turner, *Phys.Rev.*, **D26**, 2694 (1982)
- [10] P.Kernan, Ph.D. thesis, The Ohio State University (1993).  
P.Kernan, G.Steigman and T.P.Walker, in preparation.
- [11] D.Seckel, Bartol Preprint BA-93-16 hep-ph/9305311.
- [12] S.Dodelson, and M.Turner, *Phys.Rev.* **D46**, 3372 (1992)
- [13] B.D.Fields, S.Dodelson, and M.Turner, *Phys.Rev.*, **D47**,4309 (1993)

- [14] E. W. Kolb and M. S. Turner  
*The Early Universe*, Addison-Wesley (Reading, MA. 1990)
- [15] E.W. Kolb , M.S. Turner, A. Chakravorty, and D.N. Schramm, Phys. Rev. Lett. **67** 533 (1991)
- [16] M. Kawasaki, P. Kernan, H-S. Kang, R.J. Scherrer, G.Steigman and T.P. Walker, OSU-TA-5-93 (1993)
- [17] G.M. Fuller, R. A. Malaney, Phys. Rev. **D43** 3136 (1991)
- [18] L.M.Krauss, Phys.Lett.B **263**, 441 (1991)
- [19] L.M.Krauss, J.Terning and T.Applequist, Phys.Rev.Lett. **71**, 823 (1993)
- [20] S. Dodelson, and L.M. Widrow, Phys Rev. Lett. **72**, 17 (1994)
- [21] K. Jedamzik, G.M. Fuller, G.J. Mathews and T. Kajino, ASTROPH-9312066 (1994)

Table 1: Normalized Covariances

covariance of	$\eta_{10}$					
	1.00	2.00	2.50	3.00	3.40	4.00
${}^4\text{He}$ vs $\text{D} + {}^3\text{He}$	-.71	-.60	-.49	-.47	-.44	-.6
${}^4\text{He}$ vs ${}^7\text{Li}$	-.23	.04	.12	.25	.30	.25

Table 2: Correlations &  $\eta_{10}$  limits

95% C.L. $\eta_{10}$ range	$N_\nu$			
	3.0	3.025	3.04	3.05
w/ corr.	2.69 $\leftrightarrow$ 3.12	2.75 $\leftrightarrow$ 2.98	2.83 $\leftrightarrow$ 2.89	$\emptyset$
w/out corr.	2.65 $\leftrightarrow$ 3.14	2.65 $\leftrightarrow$ 3.04	2.69 $\leftrightarrow$ 2.99	2.69 $\leftrightarrow$ 2.95
sym. w/out corr.	2.62 $\leftrightarrow$ 3.17	2.63 $\leftrightarrow$ 3.10	2.65 $\leftrightarrow$ 3.03	2.66 $\leftrightarrow$ 3.00

## Figure Captions

Figure 1: BBN Monte Carlo predictions as a function of  $\eta_{10}$ . Shown are symmetric 95% confidence limits on each elemental abundance. Also shown are claimed upper limits inferred from observation.

Figure 2: Monte Carlo BBN predictions for  $Y_p$  vs  $D+{}^3He$  and allowed range for (a)  $\eta_{10} = 2.71$ , and (b)  $\eta_{10} = 3.08$ .

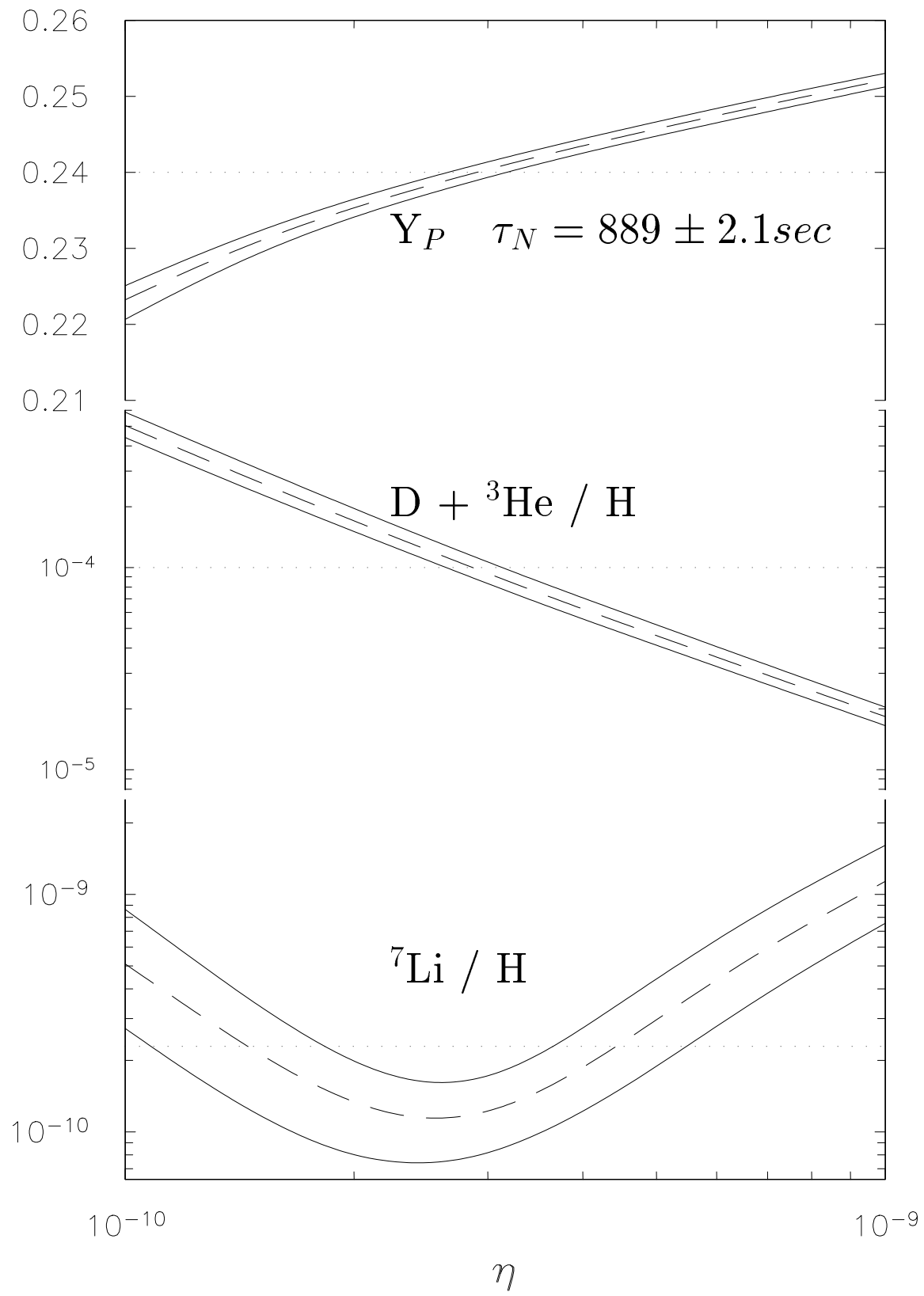
In (a) a Gaussian contour with  $\pm 2\sigma$  limits on each individual variable is also shown.

Figure 3: Number of models (out of 1000 total models)

which satisfy constraints  $Y_p \leq 24\%$  and  $D+{}^3He/H \leq 10^{-4}$  as a function of  $\eta_{10}$ , for 3.0, 3.025, 3.04, 3.05 effective light neutrino species. Curves are smoothed splines fit to the data.

This figure "fig1-1.png" is available in "png" format from:

<http://arxiv.org/ps/astro-ph/9402010v1>



This figure "fig2-1.png" is available in "png" format from:

<http://arxiv.org/ps/astro-ph/9402010v1>

This figure "fig1-2.png" is available in "png" format from:

<http://arxiv.org/ps/astro-ph/9402010v1>

